3 *Carbide Precipitation*

Carbides are largely responsible for the commercial failure of many of the early bainitic steels. The alloys could not compete against the quenched and tempered martensitic steels with their finer dispersions of carbide particles. The details of mechanical properties are discussed in Chapter 10; the purpose here is to deal with the nature and extent of carbide precipitation reactions in the context of the mechanism of the bainite transformation.

3.1 Upper Bainite

In upper bainite the carbides precipitate from austenite which is enriched in carbon; upper bainitic ferrite itself is free from precipitates (Fig. 3.1a). The most common carbide is cementite but there are notable exceptions, particularly in

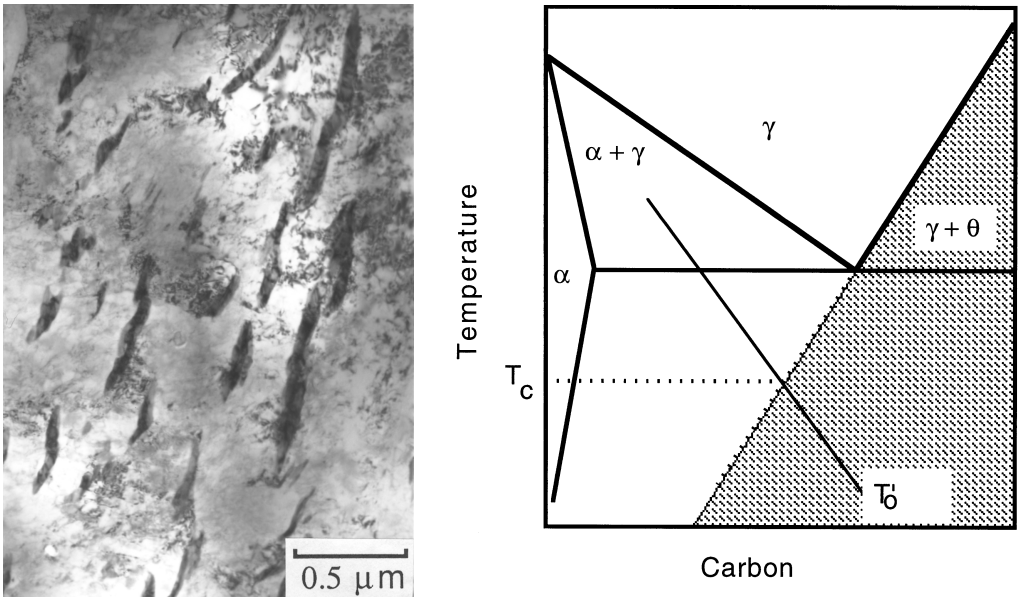

Fig. 3.1 (a) Distribution of cementite particles between the ferrite platelets in upper bainite (AISI 4340 steel). (b) Thermodynamic condition which must be satisfied before cementite can precipitate from austenite.

steels containing large concentrations of silicon. For example, the orthorhombic carbides reported by Schissler *et al*. (1975) and the *c*–carbide discovered by Sandvik (1982b), Table 3.1. Transition carbides, such as κ and the various orthorhombic forms listed in Table 3.1, only form because they are easier to nucleate, so they eventually transform into cementite.

Carbon is partitioned into the residual austenite during the bainite reaction. Cementite precipitation becomes possible when its carbon concentration x_γ exceeds the solubility limit given by the extrapolated $\gamma/(\gamma+\theta)$ phase boundary

Table 3.1 Carbides in bainite or in tempered bainite. Fe, M/C is the ratio of metal to carbon atoms. Actual lattice parameters are alloy dependent. See also a review by Yakel (1985).

Carbide	Crystal System	Fe, M/C	Reference
κ	Hexagonal $a = 6.9$ $c = 4.8$ Å	1.37	Deliry (1965) Pomey (1966)
ϵ	Hexagonal $a = 2.735$ $c - 4.339$ Å	2.4–3	Jack (1950, 1951) Hofer *et al*. (1949)
χ	Monoclinic $a = 11.563$ $b = 3.573$ Å $c = 5.058$ $\beta = 97.44^\circ$	2.2 or 2.5	Hägg (1934)
η	Orthorhombic $a = 4704$ $b = 4.318$ Å $c = 2.830$	2	Hirotsu and Nagakura (1972)
Fe_3C	Orthorthombic $a = 4.525$ $b = 5.087$ Å $c = 6.743$	3.0	
M_7C_3	Orthorhombic $a = 4.526$ $b = 7.010$ Å $c = 12.142$	7/3	Morniroli *et al*. (1983)
$(Fe, Si)C_X$	Orthorhombic $a = 8.8$ $b = 9.0$ $c = 14.4$ Å		Konoval *et al*. (1959)
$(Fe, Si)C_X$	Orthorhombic $a = 6.5$ $b = 7.7$ $c = 10.4$ Å		Schissler *et al*. (1975)
$(Fe, Si, Mn)C_X$	Orthorhombic $a = 14.8$ $b = 11.4$ $c = 8.5$ Å		Schissler *et al*. (1975)
$M_{23}C_6$	Cubic F $a = 10.621$ Å	23/6	
M_6C	Cubic F $a = 11.082$ Å	6	
c	Triclinic $a = 6.38$ $b = 5.05$ $c = 4.59$ Å $a = 90.0^\circ$ $\beta = 70.1^\circ$ $\gamma = 84.7^\circ$		Sandvik (1982b)

(Kriesement and Wever, 1956). This is illustrated in Fig. 3.1b, where the shaded area represents austenite which is unstable to the precipitation of cementite. It follows that if there are no kinetic hindrances, carbide precipitation will accompany the growth of upper bainite if the transformation temperature is below T_C (Fig. 3.1b).

The precipitation of carbides is peripheral to the formation of bainitic ferrite. On the other hand, their formation reduces the carbon concentration in the residual austenite, thus stimulating the formation of a further quantity of ferrite (designated α). Given the very small diffusion coefficients of iron and substitutional atoms at the temperatures involved (Fig. 3.2), and the absence of an incoherent interface or grain boundary to start the process, it is unlikely that this secondary ferrite forms by reconstructive transformation. Sandvik (1982b) has proposed that the decomposition of the residual austenite involves the displacive formation of a triclinic carbide, close to cementite in structure, and the subsequent formation of a small amount of *bainitic* ferrite. Nakamura and Nagakura (1986), in a study of the second stage of martensite tempering, suggested that cementite and ferrite form directly from austenite, the cementite nucleating on the ferrite/austenite boundaries and growing by rapid diffusion along this boundary. They also proposed that the secondary ferrite, which they called bainite, grows martensitically, from the carbon depleted austenite. Regions of secondary ferrite were observed to be twinned, and this was taken to indicate the formation of self–accommodating crystallographic variants of bainitic ferrite.

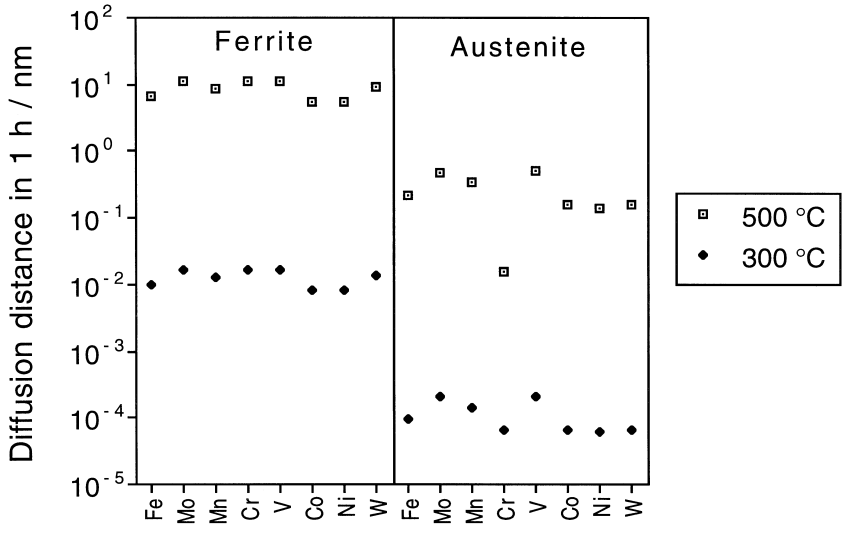

Fig. 3.2 $2(Dt)^{1/2}$ estimate of the diffusion distances for metal atoms in iron during one hour at temperature.

The sequence of reactions can be summarised as follows (α =secondary ferrite):

$$\begin{aligned} \gamma &\rightarrow \gamma + \alpha_{b,\text{supersaturated}} \\ &\rightarrow \alpha_{b,\text{unsaturated}} + \gamma_{\text{enriched}} \\ &\rightarrow \alpha_{b,\text{unsaturated}} + \alpha + \theta \end{aligned} \tag{3.1}$$

This contrasts with the cooperative growth of cementite and ferrite during the formation of pearlite in plain carbon steels:

$$\gamma \rightarrow \alpha + \theta \tag{3.2}$$

When pearlite grows in substitutionally alloyed steels, the austenite, ferrite and cementite may coexist in equilibrium over a range of temperatures, with the equilibrium compositions of all the phases changing with the temperature:

$$\gamma \rightarrow \alpha + \theta + \gamma' \tag{3.3}$$

The composition of the residual austenite (γ') is then expected to differ from that at the beginning of transformation. The reaction therefore stops before all the austenite is consumed.

In planar sections, the cementite particles in upper bainite are parallel to the habit planes of the bainitic ferrite plates. Using transmission electron microscopy, Fisher (1958) showed that these particles are in the form of irregular ribbons in three dimensions, particularly when bainite forms at high temperatures. Carbide precipitation also occurs at the austenite grain boundaries and this may influence mechanical properties, especially toughness in high strength steels (Pickering, 1958). The austenite grain boundaries are favoured heterogeneous nucleation sites so the carbides there can be expected to be coarse. When high carbon steels (> 0.45C wt%) are transformed in the bainite temperature range, there is a tendency for cementite to precipitate as thin films on the austenite grain surfaces (Stickels, 1974). These thin films are detrimental to toughness and their growth can be retarded by lowering the transformation temperature.

3.2 Lower Bainite

Lower bainite also consists of a non-lamellar aggregate of ferrite and two kinds of carbides. As in upper bainite, there is some precipitation from the enriched austenite. A finer dispersion of plate-like carbides is also found inside the ferrite plates. A common observation is that these latter carbides precipitate in a single crystallographic variant within a given ferrite plate, whereas the tempering of martensite leads to the precipitation of many variants of cementite (Fig. 3.3).

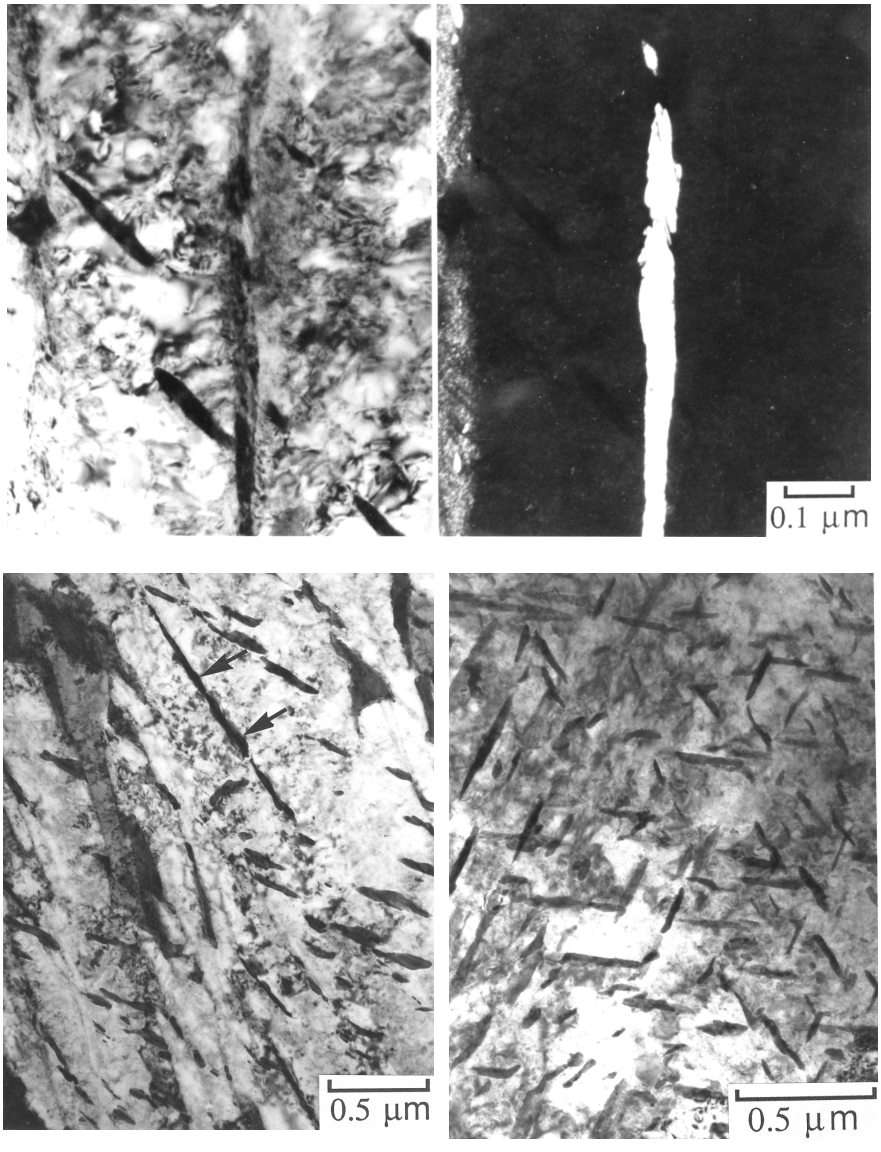

Fig. 3.3 (a–c) Fe–0.3C–4.08Cr wt%. (a) Lower bainite obtained by isothermal transformation for a short time period (435 °C, 10 min). Shows particles of cementite within the platelets but not between the platelets. (b) Corresponding dark field image showing the films of austenite between the bainitic ferrite platelets. (c) The same sample after prolonged heat treatment (435 °C, 30 min) at the isothermal transformation temperature, causing the precipitation of carbides between the ferrite platelets. (d) Typical multi-variant carbide precipitation in tempered martensite (415°C, 50 min, AISI 4340 steel). After Bhadeshia (1980a).

3.2.1 Precipitation within Lower Bainitic Ferrite

There are many observations that reveal the precipitation of carbides from supersaturated lower bainite in a process identical to the tempering of martensite. *In situ* hot-stage transmission electron microscopy has shown that the lower bainitic ferrite remains supersaturated with carbon some time after the completion of the ferrite growth (Kang *et al*., 1990).

Unlike the microstructure of tempered martensite, the carbides tend to adopt a single crystallographic variant in a given plate of lower bainite. They have their longest axes inclined at about 60° to the 'growth direction' of the ferrite platelets (ASTM, 1955; Irvine and Pickering, 1958; Speich, 1962; Shimizu and Nishiyama, 1963; Shimizu *et al*., 1964). The angle quoted must of course vary as a function of the plane of section; for lower bainitic ferrite with a habit plane $(0.761\ 0.169\ 0.626)_\gamma$, the cementite precipitates on $(1\,\bar{1}\,2)_\alpha$ giving an angle of 57° between the α and cementite habit plane normals (Bhadeshia, 1980a). Similar results have been obtained by Ohmori (1971a). In some cases, the carbides have been found to form on several different variants of the $\{1\,1\,2\}_\alpha$ plane, although a particular variant still tends to dominate (Srinivasan and Wayman, 1968b; Lai, 1975; Bhadeshia and Edmonds, 1979a). In fact, a re-examination of published micrographs sometimes reveals the presence of several variants which were not noticed in the original publication (see for example, Fig. 5, Degang *et al*., 1989).

Early experiments using Curie point measurements and dilatometry gave hints that the carbides are not always cementite (Wever and Lange, 1932; Allen *et al*., 1939; Antia *et al*., 1944). For example, the orthorhombic transition carbide discovered in high-silicon transformer steels by Konoval *et al*. (1959) has been reported to precipitate from lower bainitic ferrite in Fe–1.15C–3.9Si wt% alloy (Schissler *et al*., 1975). Nevertheless, the most common transition carbide in lower bainite is ϵ-carbide, first identified by Austin and Schwartz (1952) and subsequently confirmed by many others.

Matas and Hehemann interpreted these results to suggest that the initial carbide in hypoeutectoid bainitic-steels is ϵ, which is then replaced by cementite on holding at the isothermal transformation temperature. The rate at which the ϵ-carbide converts to cementite increases with temperature, but also depends on the steel composition. A high silicon concentration retards the reaction, as is commonly observed in the tempering of martensite (Owen, 1954; Gordine and Codd, 1969; Hobbs *et al*., 1972).

The detection of ϵ-carbide in lower bainite is important because it implies a large excess (≥ 0.25 wt%) of carbon trapped in bainitic ferrite when it first forms (Roberts *et al*., 1957). However, ϵ-carbide is not always found as a precursor to the precipitation of cementite in lower bainite. Bhadeshia and Edmonds (1979a) failed to detect ϵ-carbide in a high-silicon medium-carbon

steel (Fe–3.0Mn–2.02Si–0.43C wt%) even during the early stages of the lower bainite transformation. The steels in which ϵ-carbide has been observed during the formation of lower bainite are listed in Table 3.2.[†]

Table 3.2 Compositions of steels (wt%) in which ϵ-carbide has been found in lower bainite. The carbon concentration quoted for the alloy studied by Dubensky and Rundman represents an estimate of the concentration in the austenitic matrix of an austempered ductile cast iron.

C	Si	Mn	Ni	Cr	Mo	V	Reference
0.87	–	–	–	–	–	–	Austin and Schwartz, 1952, 1955
0.95	0.22	0.60	3.27	1.23	0.13	–	Matas and Hehemann, 1961
0.60	2.00	0.86	–	0.31	–	–	Matas and Hehemann, 1961
1.00	0.36	–	0.20	1.41	–	–	Matas and Hehemann, 1961
0.58	0.35	0.78	–	3.90	0.45	0.90	Matas and Hehemann, 1961
1.00	2.15	0.36	–	–	–	–	Deliry, 1965
0.60	2.00	0.86	–	0.31	–	–	Oblak and Hehemann, 1967
0.60	2.00	–	–	–	–	–	Hehemann, 1970
0.41	1.59	0.79	1.85	0.75	0.43	0.08	Lai, 1975
0.54	1.87	0.79	–	0.30	–	–	Huang and Thomas, 1977
0.85	2.55	0.3	–	–	–	–	Dorazil and Svejcar, 1979
0.74	2.40	0.51	–	0.52	–	–	Sandvik, 1982a
1.3	3.09	0.17	–	–	–	–	Dubensky and Rundman, 1985
0.40	2.01	–	4.15	–	–	–	Miihkinen and Edmonds, 1987a

These observations can be rationalised in terms of a theory of tempering due to Kalish and Cohen (1970), who showed that it is energetically favourable for carbon atoms to remain segregated at dislocations when compared with their presence in the ϵ-carbide lattice (Bhadeshia, 1980a). Carbon becomes trapped at dislocations and if the density of dislocations is sufficiently large, then the carbon is not available for the formation of ϵ-carbide. In such cases, precipitation of the more stable cementite occurs directly from supersaturated ferrite. Kalish and Cohen estimated that a dislocation density of $2 \times 10^{12}\,\mathrm{cm}^{-2}$ should prevent ϵ-carbide precipitation in steels containing up to 0.20 wt% carbon. This can be extrapolated to bainite bearing in mind that there are two competing reactions which help relieve the excess carbon in the ferrite: partitioning of carbon into the residual austenite and the precipitation of carbides in the

[†] ϵ-carbide has been reported in bainite produced by continuous cooling transformation, in a Fe–0.15C–0.94Mo–2.12Cr wt% steel (Baker and Nutting, 1959) and in a Fe–0.34C–1.25Mn–1.39Ni–0.34Mo wt% alloy isothermally transformed to bainite (Fondekar *et al.*, 1970). In both cases, the evidence quoted is uncertain. A study by Yu (1989) on similar steels has not revealed ϵ-carbide.

bainitic ferrite. The reactions interact since partitioning reduces the amount of carbon available for precipitation, and vice versa. Judging from available data (Table 3.2), the average carbon content of the steel must exceed about 0.55 wt% to permit the precipitation of ϵ-carbide. Otherwise, the partitioning of carbon into the austenite depletes the bainitic ferrite too rapidly to permit ϵ-carbide.

Nickel enhances the precipitation of ϵ-carbide which can therefore be obtained in bainite at lower carbon concentrations, $\simeq$0.4 wt% (Miihkinen and Edmonds, 1987a). Rao and Thomas (1980) have demonstrated a similar effect of nickel in martensitic steels; they found ϵ-carbides and cementite to be the dominant carbides during the tempering of martensite in Fe–0.27C–4Cr–5Ni and Fe–0.24C–2Mn–4Cr wt% steels respectively. Other substitutional solutes may also affect ϵ-carbide precipitation, but there are no systematic studies. As with martensite, when lower bainite is tempered, the metastable ϵ-carbide transforms to cementite and the reaction is accompanied by a volume contraction, which can be monitored accurately using dilatometry (Hehemann, 1970).

It is interesting that η-carbide (Fe_2C) has also been observed in lower bainitic ferrite obtained by transforming the austenitic matrix of a high-silicon cast iron (Franetovic *et al*., 1987a,b). This carbide has previously only been reported in tempered martensite (Hirotsu and Nagakura, 1972; Nagakura *et al*., 1983) and so reinforces the conclusion that the carbides precipitate from carbon-supersaturated lower bainitic ferrite. Like ϵ-carbide, the carbon concentration has to exceed some critical value before the η-carbide can be detected in lower bainite (Franetovic *et al*., 1987a,b).

3.2.2 *Precipitation between Lower Bainitic Ferrite Platelets*

There is no essential difference between upper and lower bainite when considering the precipitation of carbides from the carbon-enriched austenite. However, in lower bainite some of the excess carbon precipitates in the ferrite, thus reducing the quantity partitioned into the austenite (Hehemann, 1970). This in turn leads to a smaller fraction of inter-plate cementite when the austenite eventually decomposes. An important consequence is that lower bainite often has a higher toughness than upper bainite, even though it usually is stronger. The precipitation reactions for lower bainite can be summarised as follows:

Case 1: High dislocation density

$$\begin{aligned}\gamma &\rightarrow \gamma + \alpha_{b,\text{supersaturated}} \\ &\rightarrow \theta_{\text{in ferrite}} + \alpha_{b,\text{unsaturated}} + \gamma_{\text{enriched}} \\ &\rightarrow \alpha_{b,\text{unsaturated}} + \alpha + \theta_{\text{between ferrite plates}} + \theta_{\text{in ferrite}}\end{aligned} \tag{3.4}$$

Case 2: Low dislocation density

$$\begin{aligned}\gamma &\rightarrow \gamma + \alpha_{b,\text{supersaturated}} \\ &\rightarrow \epsilon_{\text{in ferrite}} + \alpha_{b,\text{unsaturated}} + \gamma_{\text{enriched}} \\ &\rightarrow \alpha_{b,\text{unsaturated}} + \epsilon_{\text{in ferrite}} + \alpha + \theta_{\text{between ferrite plates}} \\ &\rightarrow \alpha_{b,\text{unsaturated}} + \theta_{\text{in ferrite}} + \theta_{\text{between ferrite plates}} + \alpha\end{aligned} \tag{3.5}$$

κ-carbide was discovered in high-carbon steels transformed to lower bainite (Deliry, 1965; Pomey, 1966). It occurs as a transition carbide, precipitating at a late stage of the transformation, from the carbon-enriched residual austenite. The carbide has a high solubility for silicon and on continued holding at the isothermal transformation temperature, transforms to χ which in turn eventually gives way to the more stable cementite.

3.3 Kinetics of Carbide Precipitation

3.3.1 Partitioning and Distribution of Carbon

The carbon concentration of bainitic ferrite during transformation is of major importance in determining the kinetics of carbide precipitation. The transformation, however, occurs at high temperatures so excess carbon in the ferrite can be removed by precipitation or by partitioning into austenite. These two processes occur simultaneously, although one or the other may dominate depending on temperature. They can both be rapid because of the high mobility of carbon in iron.

The partitioning of excess carbon from ferrite into austenite was simulated experimentally by Matas and Hehemann (1960, 1961) who tempered mixtures of martensite and retained austenite. Single crystals of austenite were cooled below the M_S temperature (350 K) to obtain two microstructures, one containing 50% martensite and the other 90% martensite in a matrix of austenite. The crystals were then tempered at 405 K to allow the carbon to diffuse from martensite into austenite. The tempering induced the rapid precipitation of ϵ-carbide, thereby lowering the carbon concentration of the martensite to 0.22 wt%, a value consistent with that quoted by Roberts *et al*. (1957) for the equilibrium between martensite and ϵ-carbide. Continued tempering led to further reductions in the carbon concentration of the martensite as the carbon partitioned into the austenite. This partitioning occurred more rapidly for the sample containing less martensite, presumably because the larger amount of residual austenite provided a bigger sink for carbon.

The distribution of carbon in the residual austenite should not be assumed to be homogeneous after isothermal transformation to bainite (Fig. 3.4). The extent of enrichment is greater in the immediate vicinity of bainite platelets

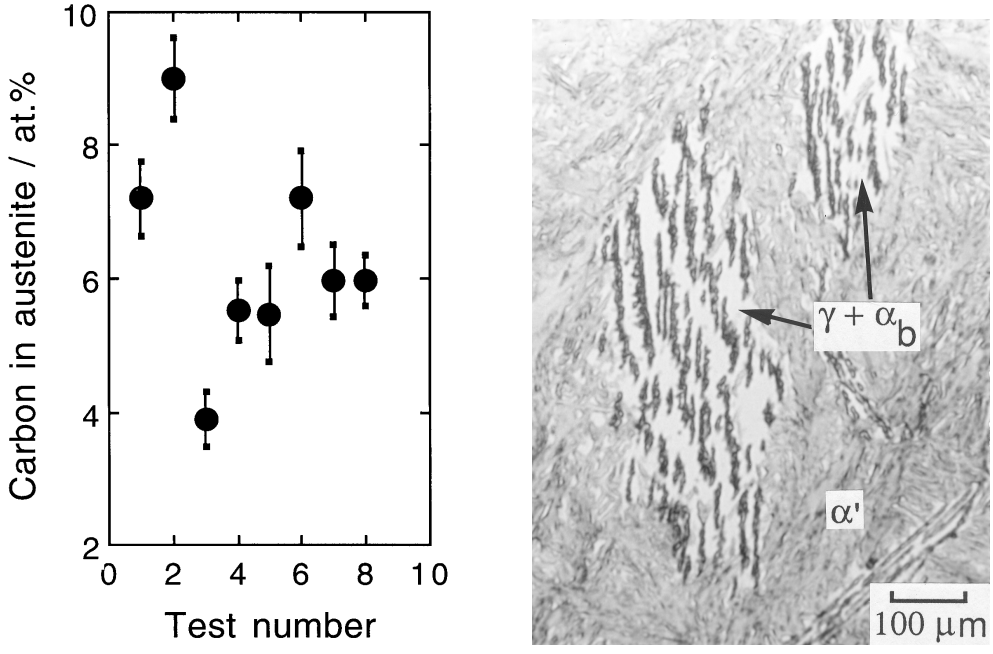

Fig. 3.4 The nonuniform distribution of carbon in the residual austenite associated with bainitic ferrite. (a) Direct measurements of the carbon concentration using an atom-probe; Fe–0.39C–2.05Si–4.08Ni wt%, isothermally transformed at 340°C for 10 h (Bhadeshia and Waugh, 1981). (b) Rim of austenite retained around a sheaf of bainite in Fe–0.81C–1.98Si–3Mn wt% steel, where the carbon concentration is expected to be largest.

or in the regions trapped between the platelets (Schrader and Wever, 1952; Matas and Hehemann, 1961). Carbon causes an expansion of the austenite so in some cases, two lattice parameters have been observed for the retained austenite, corresponding to different levels of carbon in the heterogeneous austenite within a single specimen (Matas and Hehemann, 1961). In many cases, the austenite which is relatively poor in carbon decomposes martensitically on cooling to ambient temperature. Any subsequent measurement of the carbon concentration of austenite (x_γ) using an X-ray method must then overestimate x_γ if it is assumed that the carbon was distributed uniformly in the residual austenite that existed at the isothermal transformation temperature. For example, for upper bainite in a high-silicon steel, X-ray measurements gave $x_\gamma = 1.7$ wt%, whereas volume fraction data gave an average concentration of 1.35 wt% (Houllier *et al.*, 1971).

3.3.2 *Kinetics of Precipitation from Residual Austenite*

Carbide formation lags behind that of bainitic ferrite, to an extent which depends both on the transformation temperature and on the alloy composition. In steels which transform rapidly, the delay may not be detectable. Using a chemical technique which separates precipitated carbon from that in solid solution, together with dilatometry, it has been shown that for high transformation temperatures, the amount of carbide formed is proportional to that of bainitic ferrite at any stage of the reaction (Vasudevan *et al.*, 1958). At lower temperatures, carbide precipitation follows significantly after the formation of bainitic ferrite.

With lower bainite, it is necessary to distinguish between the carbides within the bainitic ferrite which precipitate rapidly, and those which form by the slower decomposition of the carbon-enriched residual austenite (Fig. 3.3a,c). The slow rate of precipitation from austenite is due to the difference in the diffusion rates of carbon in ferrite and austenite, and because the supersaturation is larger for ferrite.

Striking evidence that the formation of carbides lags behind that of bainitic ferrite is found in silicon-rich steels. Thus, carbides do not form in upper bainite in Fe–0.31Cr–0.86Mn–2.00Si–0.60C wt% even after holding at the isothermal transformation temperature for several hours (Matas and Hehemann 1961). Similar results have been reported by Houllier *et al.*, (1971), Sandvik (1982b) and by many other researchers.

Silicon is usually present in steels as an aftermath of the deoxidation reactions involved in the steelmaking process. At large concentrations it retards the formation of cementite from austenite, making it possible to obtain a carbide-free microstructure of just bainitic ferrite and austenite (Entin, 1962; Deliry, 1965; Pomey, 1966; Hehemann, 1970; Houllier *et al.*, 1971; Bhadeshia and Edmonds, 1979a; Sandvik, 1982a,b). For the same reason, silicon favours the formation of gray cast iron with graphite instead of the cementite found in low-silicon white cast irons. It is well known that the precipitation of cementite during the tempering of martensite is significantly retarded by the presence of silicon (Bain, 1939; Allten and Payson, 1953; Owen, 1954; Keh and Leslie, 1963; Gordine and Codd, 1969; Hobbs *et al.*, 1972). This has been exploited in the design of one of the most successful ultrahigh-strength steels (commercial designation 300*M*, reviewed by Pickering, 1979).

Silicon has an incredibly low solubility in cementite. If it is forced, by the paraequilibrium transformation mechanism, to inherit the silicon as it grows then the driving force for precipitation is greatly reduced, thus retarding precipitation (Section 3.5). It was at one time thought that the retardation occurs because silicon stabilises transition carbides at the expense of

cementite (Reisdorf, 1963; Gordine and Codd, 1969) but experiments have shown that the transition carbides are not particularly enriched in silicon (Barnard *et al*., 1981).

Aluminium in solid solution also retards tempering reactions (Allten, 1954; Langer, 1968; Bhat, 1977). The effect is believed to be identical to that of silicon although detailed solubility data are not available.

Carbide-free bainitic microstructures can be obtained in steels containing little or no silicon or aluminium, for example in Fe–Cr–C alloys (Bhadeshia, 1980a), in low-carbon steels (Yang and Bhadeshia, 1987) and in copper-containing steels (Thompson *et al*., 1988). The classic '$2\frac{1}{4}$Cr1Mo' steel which is used in vast quantities in the electricity generation industry has a carbide-free bainitic microstructure. It is not yet possible to predict the effects of alloying elements on carbide precipitation reactions during the bainite transformation.

3.3.3 Kinetics of Precipitation within Bainitic Ferrite

It is particularly interesting that the precipitation of cementite from martensite or lower bainite can occur at temperatures below 400 K, in time periods too short to allow any substantial diffusion of iron atoms. The long-range diffusion of carbon atoms is of course necessary, but because carbon resides in interstitial solution, it can be very mobile at temperatures as low as 210 K (Winchell and Cohen, 1962).

The formation of cementite or other transition carbides of iron, in these circumstances of incredibly low atomic mobility, must differ from diffusional decomposition reactions. It has been believed for some time that the cementite lattice is generated by the homogeneous deformation of ferrite, combined with the necessary diffusion of carbon into the appropriate sites. In effect a displacive mechanism with paraequilibrium. The nature of the necessary displacements for generating cementite or ϵ-carbide structures have been considered phenomenologically by Andrews (1963), Hume-Rothery *et al*., (1942) and the subject has been reviewed by Yakel (1985). The models are not sufficiently developed to predict transformation kinetics except that they do no involve the diffusion of substitutional atoms and hence are consistent with rapid kinetics even at low temperatures.

The lack of atomic mobility over the temperature range where bainite grows has consequences also on the alloy carbides (such as Mo_2C) which require diffusion to grow. The size of such carbides is restricted by the distance through which the substitutional atoms can diffuse during the time scale of the experiment. This is illustrated by experiments in which the transformation of a Fe–Mo–C alloy was studied over a wide range of temperatures with the carbide type, size and composition being characterised at the highest spatial and chemical resolution possible (Stark and Smith, 1987). Fig. 3.5 shows that

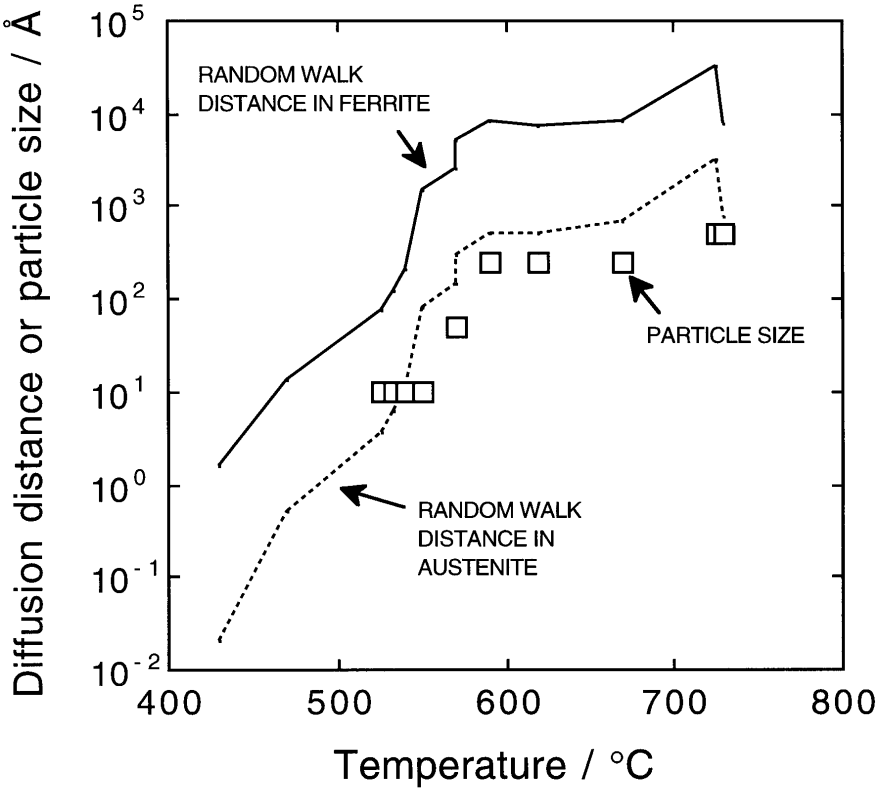

Fig. 3.5 Correlation of random walk distance for molybdenum atoms versus the measured molybdenum carbide carbide particle size (data due to Stark and Smith, 1987). The curves are the calculated $2(D_{Mo}t)^{0.5}$ values for specific heat-treatments. Molybdenum carbide was never found with bainite, only with ferrite which grew by reconstructive transformation.

the measured particle sizes correlate well with the random walk distance $2(D_{Mo}t)^{0.5}$, which is a measure of atomic mobility.

A second consequence is related to the mechanism by which the ferrite itself grows. The crystallographic change from $\gamma \rightarrow \alpha$ may occur without any diffusion. However, if the mechanism is reconstructive, then mass transport is essential during growth even when there is no change in composition (Bhadeshia, 1985b). The transformation can then only proceed at a rate consistent with this diffusion, in which case substitutional solutes like molybdenum have an opportunity to precipitate. It is noteworthy that Stark and Smith (1987) only found molybdenum carbides in ferrite which grew by a reconstructive transformation mechanism, and never in association with bainitic ferrite.

3.4 Crystallography of Carbide Precipitation in Bainite

During isothermal heat-treatments of the type used to generate bainite, the steel is not held at temperature for periods long enough to permit the long-range diffusion of substitutional atoms. Only iron carbides, such as ϵ, κ, η or cementite therefore precipitate. Other carbides which require the partitioning of substitutional solutes cannot form.

3.4.1 Cementite: Orientation Relationships

Shackleton and Kelly (1965) studied the orientation relationships between ferrite and cementite in bainite. The relationships were found to be identical to those known for cementite in tempered martensite. They most frequently observed the tempering or Bagaryatski (1950) orientation relationship:

$$\{0\,0\,1\}_\theta \| \{2\,1\,1\}_\alpha$$
$$< 1\,0\,0 >_\theta \| < 0\,\overline{1}\,1 >_\alpha$$

The next prominent α/θ orientation relationship, also found in tempered martensite, was:

$$\{0\,0\,1\}_\theta \| \{\overline{2}\,\overline{1}\,5\}_\alpha$$
$$< 1\,0\,0 >_\theta \quad \text{within } 2.6^\circ \text{ of } < 3\,\overline{1}\,1 >_\alpha$$
$$< 0\,1\,0 >_\theta \quad \text{within } 2.6^\circ \text{of } < 1\,3\,1 >_\alpha$$

In upper bainite, the large number of observed α_b/θ orientation relationships could all be derived assuming that the cementite precipitates from austenite with the Pitsch (1962) γ/θ relationship:

$$\{0\,0\,1\}_\theta \| \{\overline{2}\,2\,5\}_\gamma$$
$$< 1\,0\,0 >_\theta \quad \text{within } 2.6^\circ \text{of } < \overline{5}\,5\,\overline{4} >_\gamma$$
$$< 0\,1\,0 >_\theta \quad \text{within } 2.6^\circ \text{of } < \overline{1}\,\overline{1}\,0 >_\gamma$$

The α_b/θ relationships can be generated from the γ/θ relationship by allowing the ferrite to be a variant of the Kurdjumov and Sachs α/γ orientation relationship.

These results have been confirmed and are important in understanding the mechanism of the bainite transformation. They suggest that in lower bainite the carbides precipitate from ferrite which contains an excess of carbon. After all, precisely the same θ/α orientations are found during the tempering of martensite.

The θ/α orientation relationship found by Isaichev (1947) also occurs in lower bainite (Ohmori, 1971a; Huang and Thomas, 1977). Using rational indices, the Isaichev relationship can be expressed as follows:

$$< 0\,1\,0 >_\theta \| < 1\,\overline{1}\,\overline{1} >_\alpha$$
$$\{1\,0\,3\}_\theta \| \{1\,0\,1\}_\alpha$$

The Isaichev orientation relationship is close to that of Bagaryatskii making them difficult to distinguish using conventional electron diffraction. Accurate measurements on tempered martensite have repeatedly identified the Isaichev orientation relationship and this has led to the suggestion that the Bagaryatskii orientation does not exist (Zhang and Kelly, 1998b).

3.4.2 The Habit Plane of Cementite

Using single surface trace analysis, Shackleton and Kelly showed that for the tempering orientation relationship, the habit plane of cementite in lower bainitic ferrite is in the vicinity of the zone containing $\{1\,\overline{1}\,2\}_\alpha$ and $\{0\,\overline{1}\,1\}_\alpha$, corresponding to $\{1\,0\,1\}_\theta$ and $\{1\,0\,0\}_\theta$ respectively. The results are vague because of the irregular shape of the cementite particles and inaccuracies in the technique used. The long dimension of the cementite laths was found to be approximately $< 1\,\overline{1}\,\overline{1} >_\alpha$, corresponding to $< 0\,1\,0 >_\theta$. Note that for these data, the crystallographic indices have justifiably been quoted with respect to both the α and θ lattices since some of the trace analyses were carried out using diffraction information obtained simultaneously from both lattices. The results are consistent with the habit plane of cementite containing the direction of maximum coherency between the ferrite and cementite lattices, i.e. $< 0\,1\,0 >_\theta \parallel < 1\,\overline{1}\,\overline{1} >_\alpha$ (Andrews, 1963).

For some alloys, the observation of streaks in electron diffraction patterns has been interpreted to indicate a cementite habit of $\{0\,0\,1\}_\theta \| \{2\,1\,1\}_\alpha$ (Srinivasan and Wayman, 1968c). However, similar streaking has been observed for a cementite habit plane close to $\{2\,0\,1\}_\theta$. It is likely that the streaking is due to faulting on the $\{0\,0\,1\}_\theta$ planes (Ohmori, 1971a).

In upper bainite, the carbides precipitate from austenite and hence do not exhibit a consistent set of habit plane indices relative to ferrite. Relative to cementite the habit is close to $\{1\,0\,1\}_\theta$ with a long direction near $< 0\,1\,0 >_\theta$ (Shackleton and Kelly, 1965).

3.4.3 Three-Phase Crystallography

Crystallographic information can be interpreted in depth if the data are obtained *simultaneously* from austenite, ferrite and cementite. The first such

experiments were reported by Srinivasan and Wayman (1968b,c) and subsequent contradictory data were given by Bhadeshia (1980a). The two sets of data using *rational* indices as approximations to the measurements are as follows:

(Srinivasan and Wayman, 1968b,c)

$$[1\,1\,1]_\gamma \| [0\,1\,1]_\alpha \| [1\,0\,0]_\theta$$
$$[\bar{1}\,0\,1]_\gamma \| [\bar{1}\,\bar{1}\,1]_\alpha \| [0\,1\,0]_\theta$$
$$[1\,\bar{2}\,1]_\gamma \| [2\,\bar{1}\,1]_\alpha \| [0\,0\,1]_\theta$$

(Bhadeshia, 1980a)

$$[1\,1\,1]_\gamma \| [0\,1\,1]_\alpha$$
$$[0\,\bar{1}\,1]_\gamma \| [\bar{1}\,\bar{1}\,1]_\alpha$$

$$[0\,\bar{1}\,1]_\alpha \| [1\,0\,0]_\theta$$
$$[1\,\bar{1}\,\bar{1}]_\alpha \| [0\,1\,0]_\theta$$
$$[2\,1\,1]_\alpha \| [0\,0\,1]_\theta$$

For the first set of data, the habit plane of the cementite within the lower bainitic ferrite is found to be $(1\,1\,2)_\alpha$, corresponding to $(1\,0\,1)_\gamma$. Srinivasan and Wayman noted that this coincides with the presumed lattice-invariant deformation of lower bainite, implying that this somehow explains the single crystallographic variant of cementite in lower bainite, as compared with the many found when martensite is tempered. When the lattice-invariant deformation is slip, as is the case for bainite, it is incredibly difficult to establish any microstructural evidence in its support (although Ohmori, 1989, has claimed that the cementite traces in lower bainite can often be seen to be parallel to the traces of transformation twins in adjacent and approximately parallel plates of martensite). Srinivasan and Wayman interpreted the presence of the carbide on the appropriate planes to lend support to proposed mode of lattice invariant deformation in bainite. It was pointed out that the results may not be generally applicable, because they found that for a Fe–3.32Cr–0.66C wt% alloy the cementite habit plane seemed to be $\{0\,0\,1\}_\theta$ unlike the case for the richly alloyed sample.

Unfortunately, the second set of data above (Bhadeshia, 1980a) is not in agreement with the Srinivasan and Wayman hypothesis, and they noted themselves that the cementite habit plane in another Fe–Cr–C alloy containing less chromium and carbon was $(0\,0\,1)_\theta$ rather than $(0\,1\,0)_\theta$. Thus, although the lattice-invariant deformation may be linked to the nucleation of cementite under some circumstances, it does not provide a consistent explanation in

others. It also does not explain why multiple variants of carbides are observed in martensites.

3.4.4 Interphase Precipitation

An alternative view is that the cementite of lower bainite nucleates and grows at the austenite-ferrite interface, a process which is well established in the high temperature precipitation of carbides and is described as *interphase precipitation* (Honeycombe and Pickering, 1972). The carbon that is necessary to sustain the growth of cementite can be absorbed from the adjacent austenite and it is then not necessary for the ferrite to be supersaturated. It is argued that during nucleation, the cementite should adopt an orientation which provides good lattice matching with *both* α and γ. If it happens to be the case that there is only one orientation in space which allows good matching with both the adjacent phases, then the theory indicates that only one crystallographic variant of cementite should precipitate for a given variant of ferrite.

It seems intuitively reasonable that a particle at the transformation interface should attempt to lattice match simultaneously with both the adjacent phases. However, the experimental evidence quoted in support of the model (reviewed by Honeycombe, 1984) is inadequate. For example, during the interphase precipitation of $M_{23}C_6$ in chromium-rich steels, the carbide (which has a face-centred cubic lattice) adopts a cube-cube orientation with the austenite, and a Kurdjumov–Sachs orientation with the ferrite. However, $M_{23}C_6$ in austenite always precipitates in a cube–cube orientation with austenite, even in the absence of any ferrite. Suppose that the carbide precipitates in austenite, and that the austenite then transforms to ferrite, then it follows that the ferrite is likely to adopt a rational Kurdjumov–Sachs type orientation with the austenite, and *consequently* with the $M_{23}C_6$, the final three phase crystallography having nothing to do with simultaneous lattice matching between all three phases.

During interphase precipitation, the $M_{23}C_6$ could be completely oblivious of the ferrite, even though it may be in contact with the phase, but the good three phase crystallography would nevertheless follow simply because the $M_{23}C_6$ has a cube–cube orientation with the austenite. To test unambiguously, the theory requires a system where the particles which form at the interphase interface are able to adopt many different variants of an orientation relation with the austenite. It is suggested that interphase precipitation of Mo_2C is an example suitable for further work.

Given a Bagaryatskii orientation relationship between lower bainitic ferrite and its internal cementite particles, and a Kurdjumov–Sachs orientation relationship between the ferrite and austenite, it can be shown (Bhadeshia, 1980a) that the three phase crystallography expected on the basis of the lattice matching arguments is:

$$[1\,0\,0]_\theta \| [0\,\overline{1}\,1]_\alpha \| [1\,1\,1]_\gamma$$
$$[0\,1\,0]_\theta \| [1\,\overline{1}\,\overline{1}]_\alpha \| [\overline{1}\,0\,1]_\gamma$$

The experimental data for lower bainite are inconsistent with these orientation relations, the cementite failing to lattice match with the austenite. This conclusion remains if the α/γ orientation relationship is of the Nishiyama-Wasserman type.

There is another way of verifying this conclusion. Aaronson *et al*. (1978) have modelled the growth of cementite which nucleates at the α/γ interface. In this model, the penetration of the cementite into the adjacent ferrite or austenite is determined by the rate at which either of these phases transform into cementite. The growth of the cementite is treated in terms of a one-dimensional diffusion-controlled growth process. With the Zener approximation of a linear concentration gradient in the parent phase, the penetration of cementite in ferrite (G_α) and in austenite (G_γ) are given by:

$$G_\alpha \simeq \frac{1}{2}\left(\frac{D_\alpha}{t}\right)^{\frac{1}{2}} \frac{(\overline{c}^\alpha - c^{\alpha\theta})}{[2(c^{\theta\alpha} - c^{\alpha\theta})(c^{\theta\alpha} - \overline{c})]^{\frac{1}{2}}} \tag{3.6}$$

$$G_\gamma \simeq \frac{1}{2}\left(\frac{D_\gamma}{t}\right)^{\frac{1}{2}} \frac{(\overline{c}^\gamma - c^{\gamma\theta})}{[2(c^{\theta\gamma} - c^{\gamma\theta})(c^{\theta\gamma} - \overline{c})]^{\frac{1}{2}}} \tag{3.7}$$

where D_α is the diffusivity of carbon in ferrite, $\overline{c}$ is the average carbon concentration in the parent phase (α or γ), $c^{\gamma\theta}$ represents the concentration of carbon in the austenite which is in equilibrium with cementite and t represents the time after the nucleation event. If it is assumed that $c^{\theta\alpha}$ or $c^{\theta\gamma}$ are much greater than $\overline{c}$, $c^{\alpha\theta}$ or $c^{\gamma\theta}$, the ratio of growth rates is given by:

$$\frac{G^\alpha}{G^\gamma} = \frac{D_\alpha^{\frac{1}{2}}(\overline{c}^\alpha - c^{\alpha\theta})}{D_\gamma^{\frac{1}{2}}(\overline{c}^\gamma - c^{\gamma\theta})} \tag{3.8}$$

Note that the left hand side of this equation could be replaced by the corresponding ratio of particle dimensions in the two parent phases. Aaronson *et al*., made the further assumption that the carbon concentrations of the austenite and ferrite before the onset of cementite formation are given by $c^{\gamma\alpha}$ and $c^{\alpha\gamma}$ respectively. This in turn implies a number of further assumptions which are not consistent with experimental data: that carbide formation does not begin until the formation of all bainitic ferrite is complete, that there is no supersaturation of carbon in the bainitic ferrite and that the bainite transformation does not obey the incomplete-reaction phenomenon.

On the basis of these assumptions, the cementite in bainite essentially grows by drawing on the richer reservoir of carbon in the austenite, and should

therefore penetrate to a far greater extent into the austenite than into the ferrite. Contrary to this conclusion, direct observations prove that in the rare cases where a cementite particle in lower bainite happens to be in contact with the transformation interface, the cementite is confined to the ferrite (Bhadeshia, 1980a).

Aaronson *et al*. also concluded that since the model predicts that the interphase growth of cementite occurs into both bainitic ferrite and austenite, the debate about whether the carbides nucleate in α or γ is irrelevant. This is not justified because it assumes that the carbides nucleate at the interphase interface, whereas it is more likely that the carbides which precipitate within the lower bainitic ferrite nucleate and grow from the supersaturated bainitic ferrite.

3.4.5 Relief of Strain Energy

The evidence suggests that the occurrence of a single crystallographic variant of carbide in lower bainite cannot be explained in terms of either the interphase precipitation model or the lattice-invariant shear arguments. A possible alternative explanation is that the variant which forms is one that is best suited towards the relief of elastic strains associated with the austenite to lower bainite transformation (Bhadeshia, 1980a). The observation that carbide precipitation modifies the surface relief of lower bainite supports this conclusion, particularly since freshly formed plates, apparently without carbide precipitation, exhibit perfect invariant-plane strain relief (Clark and Wayman, 1970).

If this explanation is accepted, then it begs the question as to why multiple variants of carbides occur during the tempering of martensite. However, an examination of a large number of published micrographs in the literature indicates that even in tempered martensite, there is usually one dominant variant and in many cases, just one variant of carbide present. Examples can be found in standard textbooks such as that by Honeycombe (Fig. 8.3, 1981), or in research articles (Speich, Fig. 3, 1987).

3.4.6 Epsilon-Carbide

The orientation relationship between ϵ-carbide in tempered martensite was deduced by Jack (1950, 1951) as:

$$(1\,0\,1)_\alpha \| (1\,0\,\bar{1}\,1)_\epsilon$$
$$(2\,\bar{1}\,1)_\alpha \| (1\,0\,\bar{1}\,0)_\epsilon$$
$$(0\,1\,1)_\alpha \| (0\,0\,0\,1)_\epsilon$$
$$(\bar{1}\,\bar{1}\,1)_\alpha \| (1\,\bar{2}\,1\,0)_\epsilon$$

which also implies that:

$$(1\,0\,1)_\alpha \simeq 1.37^\circ \text{ from } (1\,0\,\bar{1}\,1)_\epsilon$$
$$[1\,0\,0]_\alpha \simeq 5^\circ \text{ from } [1\,1\,\bar{2}\,0]_\epsilon$$

The very same orientation relationship is also found for ϵ-carbide in lower bainite (Huang and Thomas, 1977). The carbide is in the form of plates which are approximately 6–20 nm thick and 70–400 nm long and possess a ragged interface with the matrix. Single-surface trace analysis suggests that on average the particles grow along $< 1\,0\,0 >_\alpha$ directions on $\{0\,0\,1\}_\alpha$ habit planes (Lai, 1975).

It has been suggested by Huang and Thomas that ϵ-carbides precipitates at the austenite/bainite interface, because its orientation with the ferrite can be generated by assuming a Kurdjumov–Sachs α/γ orientation, and an ϵ/γ relationship in which

$$\begin{aligned}(1\,1\,1)_\gamma &\| (0\,0\,0\,1)_\epsilon \\ (1\,\bar{1}\,0)_\gamma &\| (1\,\bar{2}\,1\,0)_\epsilon\end{aligned} \tag{3.9}$$

However, the three phase crystallography is not unique and hence does not explain the observed single variant of carbide in lower bainite.

During the prolonged ageing of bainite, Sandvik (1982a) found that small regions of austenite retained within bainite sheaves transform into ϵ carbide, with the three-phase crystallography described by Huang and Thomas. The observed ϵ-carbide habit plane, $(1\,0\,1)_\alpha \| (0\,0\,0\,1)_\epsilon$ is different from that claimed by Lai.

The orientation relationship expected between ϵ-carbide and austenite has until recently been a matter of speculation. The carbide has now been found to precipitate directly in austenite in high-carbon cast iron with the orientation relationship stated in equation 3.9 (Gutierrez *et al*., 1995). The precipitates are in the form of fine, coherent particles homogeneously distributed throughout the austenite and form in at least three variants of the orientation relationship (Fig. 3.6). When the austenite transforms to martensite, only two of these variants adopt the Jack orientation relationship with the martensite.

3.4.7 Eta-Carbide

η-carbide is a transition Fe_2C carbide in the orthorhombic crystal system. It is usually associated with the tempering of martensite (Hirotsu and Nagakura, 1972; Nagakura *et al*., 1983) where the martensite/carbide orientation relationship is found to be as follows:

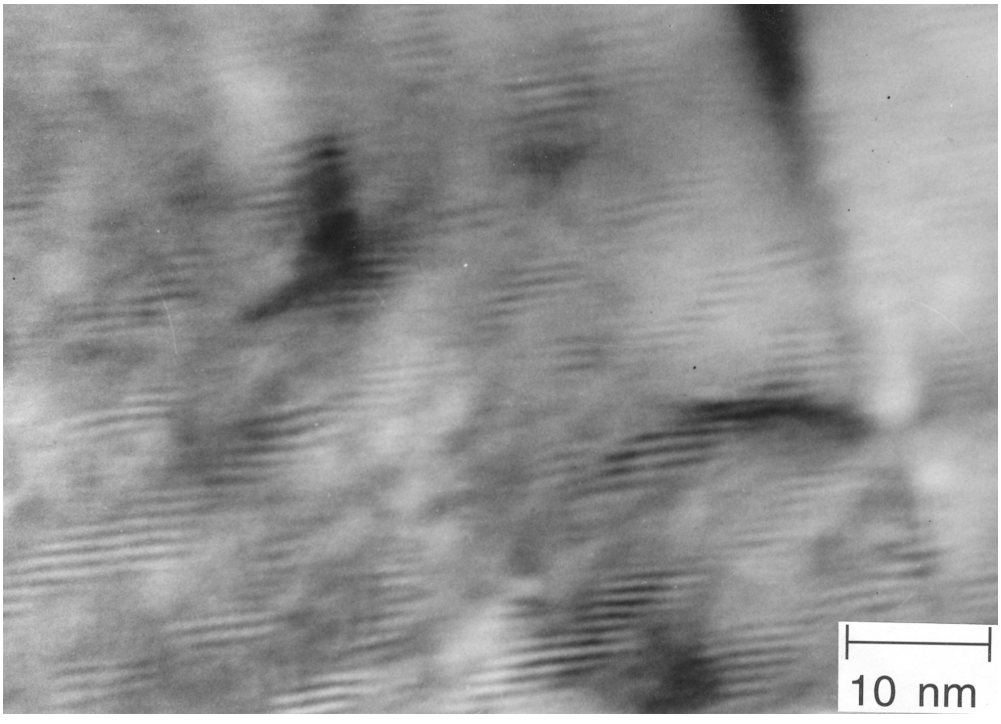

Fig. 3.6 The homogeneous precipitation of ϵ-carbide in austenite (Gutierrez *et al.*, 1995).

$$(1\,1\,0)_\eta \| \{0\,1\,0\}_\alpha$$
$$[0\,0\,1]_\eta \| < 1\,0\,0 >_\alpha$$

The carbide has been observed in lower bainite in grey cast iron, where electron diffraction confirms that (Franetovic *et al.*, 1987a,b):

$$[0\,0\,1]_\eta \| < 1\,0\,0 >_\alpha \| < 0\,\bar{1}\,1 >_\gamma$$

This information is consistent with the η-carbide/martensite orientation relationship stated earlier and lends further support to the hypothesis that the carbides within lower bainitic ferrite precipitate in a manner analogous to the tempering of martensite.

3.4.8 Chi-Carbide

χ-Carbide is another transition carbide which is metastable with respect to cementite. It is found during the tempering of martensite, where high-resolution electron microscopy has demonstrated that what at first sight appears to be faulted cementite in fact consists of interpenetrating layers of

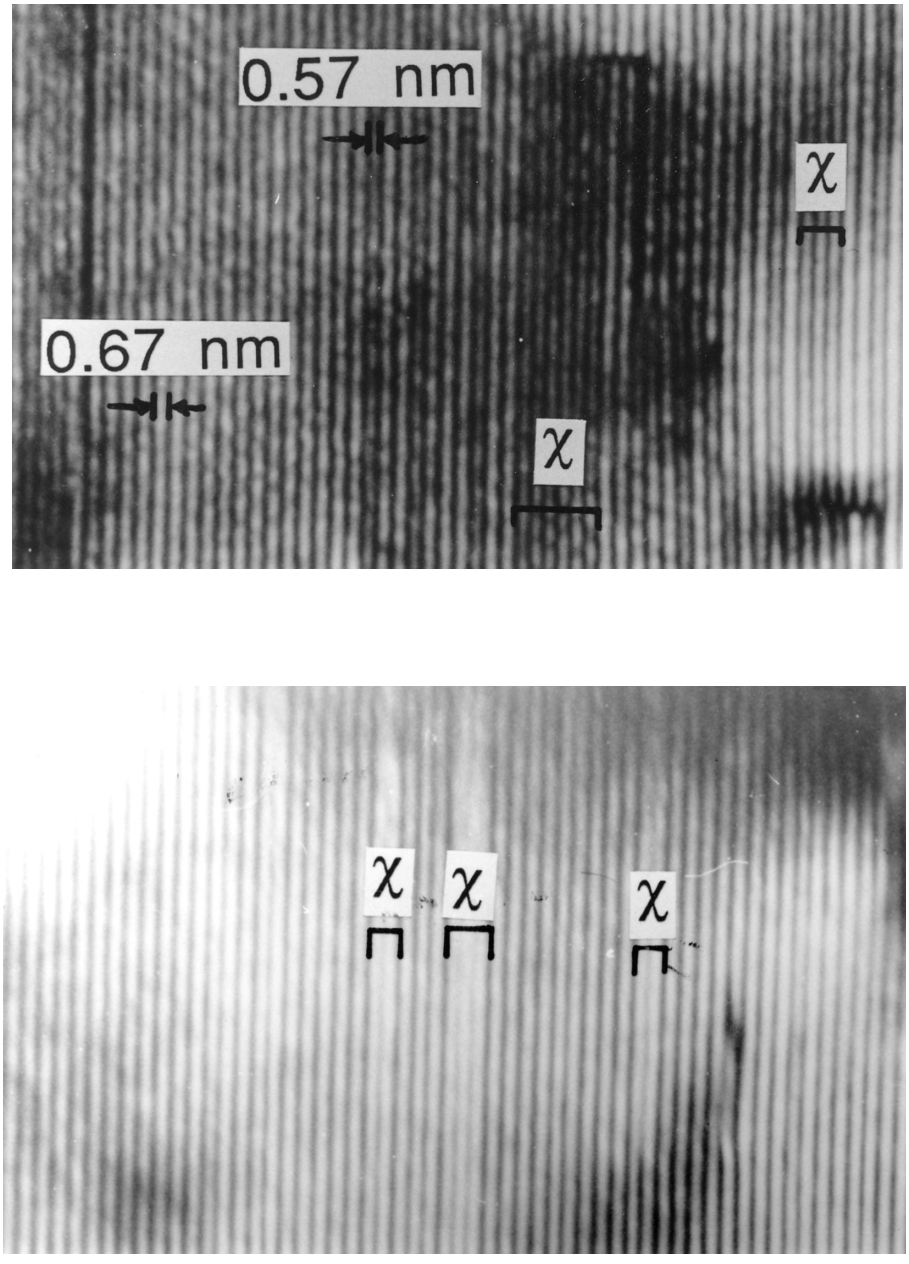

Fig. 3.7 Lattice resolution transmission electron micrographs showing the intergrowth of layers of cementite and χ-carbide (Ohmori, 1986). (a) Carbide particle which precipitated in lower bainitic ferrite; (b) carbide particle formed during the tempering of martensite.

cementite and χ, described as *microsyntactic intergrowth* (Nagakura *et al*., 1981; Nakamura *et al*., 1985). The $\{2\,0\,0\}_\chi$ planes are found to be parallel to the $\{0\,0\,1\}_\theta$ planes of different spacing (0.57 and 0.67 nm respectively). Thus, the faults in the cementite really correspond to regions of χ, each a few interplanar spacings thick, and this intimate mixture of cementite and χ consequently has a nonstoichiometric overall composition expressed by $Fe_{2n+1}C_n$, where $n \geq 3$.

Similar observations have been reported by Ohmori (1986), but for cementite in both tempered martensite and lower bainite, in a Fe–0.7C wt% steel (Fig. 3.7). In both cases, high-resolution electron microscopy (HREM) revealed that the cementite particles contained regions of χ-carbide, lending yet more support to the analogy between tempered martensite and lower bainite. This is consistent with Ohmori's observation that cementite in bainitic ferrite increases in size during transformation, as if growing from carbon supersaturated ferrite.

Ohmori (1986) has also claimed that the mechanism of precipitation in the lower bainite was different from that in tempered martensite, on the grounds that the cementite in the lower bainite contained a smaller amount of χ-carbide. A difficulty with this conclusion is that the amount of material examined in an HREM experiment is so small that it is unlikely to be representative. The heat-treatments utilised in producing lower bainite and martensite are also different making valid comparisons difficult.

Direct observations on martensite tempering, by Nakamura *et al*. (1985), indicate that the mechanism by which the mixed χ/cementite particles are replaced by cementite can be complicated and site dependent. One of the cementite layers in the mixed particle tends to grow into the surrounding matrix, at the expense of the mixed particle which dissolves. This dissolution is found to occur more rapidly for mixed particles which happen to be located at grain boundaries, presumably because such boundaries provide easy diffusion paths.

It is interesting that the mechanism involves the dissolution of both the cementite and χ in the mixed particles. This might be expected if it is assumed that the original particle forms by displacive transformation; the accompanying strain energy could then provide the driving force for its replacement by more globular cementite particles forming by reconstructive growth. Also, the boundaries between the χ and cementite layers are coherent and would not be expected to be very mobile, in which case, the cementite layers would be kinetically hindered from growing into the adjacent χ layers.

3.5 Chemical Composition of Bainitic Carbides

It has long been established, using magnetic, chemical and X-ray methods on extracted carbides, that the cementite associated with upper bainite has a substitutional solute content which is close to, or slightly higher than that of

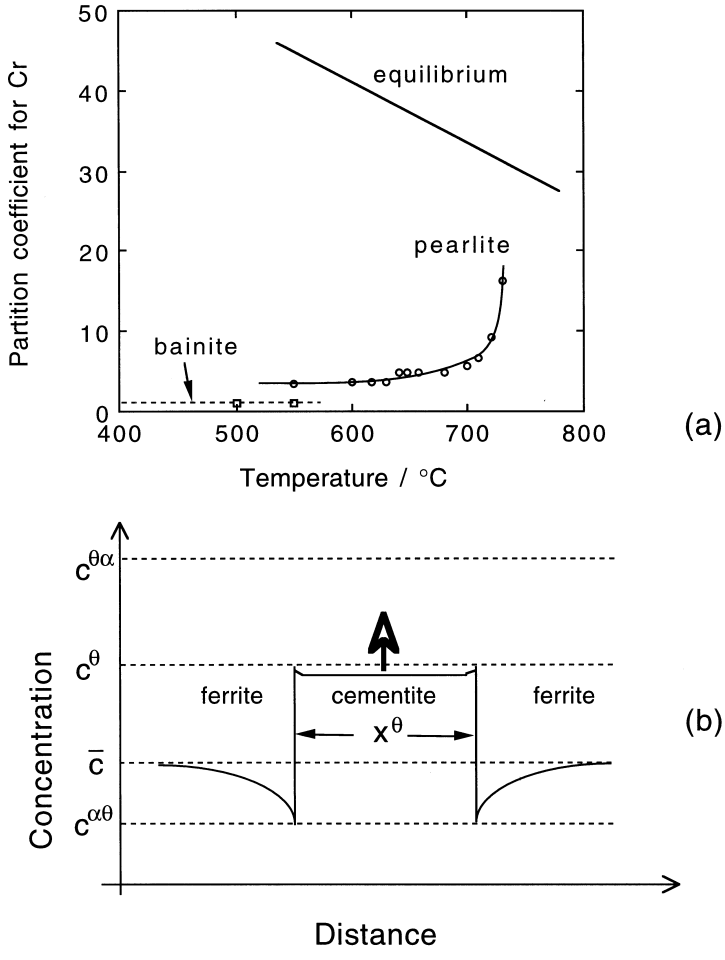

Fig. 3.8 (a) The partition coefficient for chromium in cementite, when the cementite is a part of bainite or pearlite, together with equilibrium data (Chance and Ridley, 1981). The partition coefficient is the ratio of the concentration in cementite to that in the ferrite. (b) The concentration profile that develops during the enrichment of a cementite particle.

the steel as a whole. This is not expected from considerations of chemical equilibrium (see for example, Hultgren, 1947, 1953).

Tsivinsky *et al*. (1959) reported that chromium and tungsten partitioned from austenite into cementite during the growth of pearlite, but not during that of bainite. Chance and Ridley (1981) found that for upper bainite in a Fe–0.81C–1.41Cr wt% alloy, the partition coefficient k_{Cr}, defined as (wt% Cr in θ)/(wt% Cr in α) could not be distinguished from unity (Fig. 3.8). Chance and Ridley

suggested that partitioning occurs during the pearlite reaction but at the same temperature does not occur with bainite because there is a fast diffusion path along the incoherent interface for pearlite.

These and other results provide compelling evidence that the carbides which form during the bainite reaction or indeed during the tempering of martensite grow by a displacive mechanism. Such a mechanism must naturally involve the diffusion of carbon, but not of substitutional solutes or iron atoms. It is particularly interesting that the precipitation of cementite from martensite or lower bainite can occur under conditions where the diffusion rates of iron and substitutional atoms are incredibly small compared with the rate of precipitation (Fig. 2.12). The long-range diffusion of carbon atoms is of course necessary, but because of its interstitial character, substantial diffusion of carbon remains possible even at temperatures as low as $-60\,^{\circ}\mathrm{C}$. The Fe:X ratio thus remains constant everywhere and subject to that constraint, the carbon achieves equality of chemical potential; the cementite is then said to grow by *paraequilibrium* transformation.

High-resolution evidence supporting the idea that the carbide particles grow by paraequilibrium displacive transformation has been published by Sandvik (1982b), Nakamura and Nagakura (1986) and Taylor *et al*. (1989a,b). In recent work it has been confirmed that the initial composition of the cementite precipitated during the tempering of martensite is not affected by the heterogeneous nucleation site, whether that is at plate boundaries or within the plates themselves (Thomson and Miller, 1995; Ghosh *et al*., 1999).

In a remarkable experiment, Babu *et al*. (1993) have shown using the atom-probe technique that the cementite obtained by tempering martensite is forced to inherit the silicon concentration of the martensite. They did not find any redistribution of substitutional solutes even on the finest conceivable scale; the atom-probe technique has single atom resolution for both chemical and spatial analysis (Fig. 3.9). The results rule out the possibility of local equilibrium at the interface and conclusively establish the paraequilibrium mode of cementite precipitation. The fact that silicon is trapped by cementite is important given that its equilibrium solubility in cementite is virtually zero. It follows from this that the trapped species such as Si must partition with prolonged heat treatment and this is precisely what is observed experimentally (Babu *et al*.).

To summarise, substitutional solute atoms are trapped in the cementite when the latter precipitates in bainite or martensite. That is, the cementite forms by a paraequilibrium transformation mechanism. In silicon-containing steels the free energy change associated with the paraequilibrium precipitation of cementite must be much smaller than when the cementite is free of silicon. It is probable that this is what leads to suppression of cementite in high-silicon bainitic or martensitic steels.

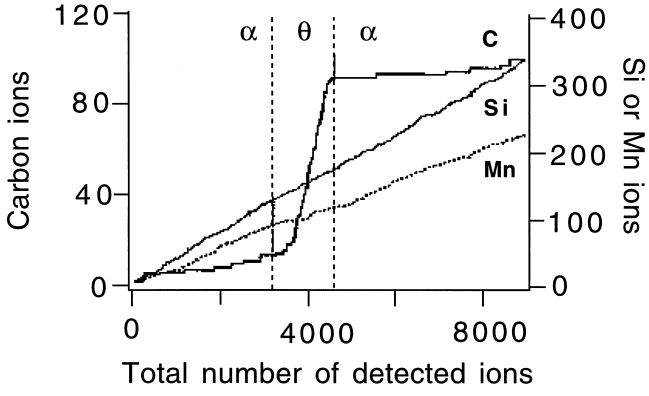

Fig. 3.9 The results of an atomic resolution chemical analysis experiment across a pair of ferrite/cementite (α/θ) interfaces. Any changes in composition are represented by a change in the slope. It is evident that there is no partitioning of silicon or manganese when cementite precipitates from martensite. The alloy used has the chemical composition Fe–1.84C–3.84Si–2.95Mn at%, and was tempered at 350 °C for 30 min (Babu *et al.*, 1993).

The response of carbides to a stress applied during the precipitation process can reveal further information about their mechanism of formation; this will be discussed in Chapter 8.

3.6 Summary

The growth of upper bainite leads to the partitioning of carbon into the residual austenite. If the transformation conditions render the austenite thermodynamically unstable with respect to carbide precipitation, then it eventually decomposes by the precipitation of cementite and more ferrite. In some alloys, cementite formation is preceded by that of transition iron-carbides such as κ or χ. In lower bainite, some of the carbon precipitates from supersaturated ferrite and the rest is partitioned into the remaining austenite. The quantity of carbides that precipitate from the austenite is therefore smaller when compared with upper bainite. Every carbide precipitation reaction that is found in tempered martensite has also been observed in lower bainite with exactly identical crystallographic and morphological characteristics. One difference is that the carbide particles in any given lower bainitic plate tend to precipitate in a single crystallographic orientation whereas the tempering of martensite usually leads to many crystallographic variants. This is because the self-stress of a lower bainite plate favours precipitation of a particular carbide variant, and this

effect is prominent in bainite where the driving force for carbide precipitation is smaller than that associated with the tempering of martensite.

The carbide precipitation reactions for both upper and lower bainite are secondary events which occur after the growth of bainitic ferrite. In some alloys, especially those containing large concentrations of silicon or aluminium, the carbide precipitation reaction can be so sluggish that for practical purposes, the bainite consists of a mixture of only bainitic ferrite and carbon-enriched residual austenite.

The mobility of atoms over the range of temperatures within which bainite grows is extraordinarily small. This and other observations suggest that the carbides grow by a displacive mechanism in which only the interstitial elements diffuse. This is consistent with the fact that there is no change in substitutional solute content when bainitic carbides precipitate, and with the crystallography of carbide precipitation.